16

Principles of Neutron Coincidence Counting

N. Ensslin

16.1 INTRODUCTION

The quantity of uranium or plutonium present in bulk samples of metal, oxide, mixed-oxide, fuel rods, etc., can often be assayed nondestructively by neutron coincidence counting. This powerful technique exploits the fact that neutrons from spontaneous fission or induced fission are emitted essentially simultaneously. In many cases it is possible to obtain a nearly unique signature for a particular nuclear material. The measurement can be made in the presence of neutrons from room background or (α,n) reactions because these neutrons are noncoincident, or random, in their arrival times.

Table 11-1 in Chapter 11 summarizes the spontaneous fission neutron yields and multiplicities of many isotopes important in the nuclear fuel cycle. For plutonium, the table shows that ^{238}Pu, ^{240}Pu, and ^{242}Pu have large spontaneous fission yields. For uranium, there are no large yields; however, ^{238}U in kilogram quantities will have a measurable yield. Spontaneous fission is usually accompanied by the simultaneous emission of more than one neutron. Thus an instrument that is sensitive only to coincident neutrons will be sensitive only to these isotopes. The quantity of these particular isotopes can be determined even if the chemical form of the material yields additional single neutrons from (α,n) reactions. Then, if the isotopic composition of the material is known, the total quantity of plutonium or uranium can be calculated.

For a plutonium sample containing ^{238}Pu, ^{240}Pu, and ^{242}Pu, the observed coincidence response will be due to all three isotopes. However, ^{240}Pu is usually the major even isotope present in both low-burnup plutonium (~6% ^{240}Pu) and high-burnup, reactor-grade plutonium (~15 to 25% ^{240}Pu). For this reason it is convenient to define an effective ^{240}Pu mass for coincidence counting by

$$^{240}Pu_{eff} = 2.52\ ^{238}Pu + {}^{240}Pu + 1.68\ ^{242}Pu \quad . \tag{16-1}$$

Plutonium-240(eff) is the mass of ^{240}Pu that would give the same coincidence response as that obtained from all the even isotopes in the actual sample. Typically, $^{240}Pu_{eff}$ is 2 to 20% larger than the actual ^{240}Pu content. The coefficients 2.52 and 1.68 are determined by (a) the relative spontaneous fission half-lives of each isotope (Table 11-1), (b) the relative neutron multiplicity distributions of each isotope (Table 11-2), and (c) the manner in which these multiplicities are processed by the coincidence circuitry (see for example Ref. 1). The relative spontaneous fission yields are the dominant effect. The coefficients given above are appropriate for the shift register circuitry described later in this chapter, but would change only slightly for other circuits.

Passive counting of spontaneous fission neutrons is the most common application of neutron coincidence counting. However, because fission can be induced, particularly in fissile isotopes such as ^{239}Pu and ^{235}U, a sample containing large quantities of fissile isotopes can be assayed by coincidence counting of induced fissions. The induced coincidence response will be a measure of the quantity of fissile isotopes present. If the fissions are induced by an (α,n) neutron source, the coincidence circuit can discriminate the induced correlated signal from the uncorrelated source.

Passive and active neutron coincidence counters have found many applications in domestic and international safeguards, as described in Chapter 17. Coincidence counters are usually more accurate than total neutron counters because they are not sensitive to single neutrons from (α,n) reactions or room background. However, the total neutron count rate can provide information that complements the coincidence information. For a wide range of material categories, it is generally useful to measure both the coincidence response and the total neutron response.

16.2 CHARACTERISTICS OF NEUTRON PULSE TRAINS

As an aid to understanding coincidence counting it is helpful to consider the train of electronic pulses produced by the neutron detector. These electronic pulses, each representing one detected neutron, constitute the input to the coincidence circuit. This input can be thought of either as a distribution of events in time or as a distribution of time intervals between events, whichever is more convenient. In any case, the observed distribution is produced by some combination of spontaneous fissions, induced fissions, (α,n) reactions, and external background events. As mentioned in Section 16.1, fission events usually yield multiple neutrons that are correlated or coincident in time, whereas (α,n) reactions and background events yield single neutrons that are uncorrelated or random in time.

16.2.1 Ideal and Actual Pulse Trains

An ideal neutron pulse train containing both correlated and uncorrelated events might look like train (a) in Figure 16.1. An actual pulse train detected by a typical

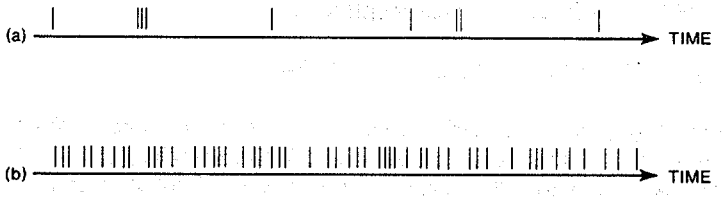

Fig. 16.1 *Neutron pulse trains as they might appear on a time axis. (a) An idealized pulse train containing correlated and uncorrelated events. (b) An actual pulse train observed at high counting rates using a detector with typical efficiency and die-away-time characteristics.*

neutron coincidence counter will look more complex, as shown by train (b) in Figure 16.1. This is because the neutron coincidence counter design affects the pulse train in several ways.

First, large samples can usually be accommodated in the central well of the coincidence counter. One kilogram of plutonium containing 20% ^{240}Pu will emit about 200 000 n/s. If the coincidence counter has a typical detection efficiency of 20%, the total neutron count rate will be 40 000 n/s, and the mean time interval between detected events will be 25 μs. Second, the typical efficiency $\varepsilon = 20\%$ of a coincidence counter is substantially less than 100%, so that the majority of emitted neutrons are not detected. Most spontaneous fissions are also not detected. If n coincident neutrons are emitted, the probability of detecting k is given by

$$P(n,k) = \frac{n!}{(n-k)!\,k!}\,\varepsilon^k(1-\varepsilon)^{n-k} \quad . \tag{16-2}$$

If in this example two neutrons were emitted (close to the mean spontaneous fission multiplicity of 2.16 for ^{240}Pu), the probability P(2,0) of detecting no neutrons is 0.64. The probability P(2,1) of detecting one neutron is 0.32 and the probability P(2,2) of detecting two neutrons is 0.04. Thus more than half of all fission events are never detected, and most of those that are detected register only one neutron. Actual detected bursts of two or more neutrons are relatively rare, occurring only 4% of the time in the above example. Third, many of the apparent coincidences in the observed pulse train will be due to accidental overlaps of background events, background and fission events, or different fission events.

A fourth important effect is the finite thermalization and detection time of the neutrons in the polyethylene body of the well counter. The process of neutron moderation and scattering within the counter can require many microseconds of time. At any moment the process can be cut short by absorption in the polyethylene, the detector tube, or other materials, or by leakage out of the counter. The process can also be prolonged by neutron-induced fission leading to additional fast neutrons that undergo moderation and scattering before they in turn are absorbed. As a consequence of all of these processes, the neutron population in the counter dies away with time in a complex, gradual fashion after a spontaneous fission occurs. To a good approximation this die-away can be represented by a single exponential:

$$N(t) = N(0)\,e^{-t/\tau} \tag{16-3}$$

where N(t) is the neutron population at time t, and τ is the mean neutron lifetime in the counter, the die-away time. Die-away times are determined primarily by the size, shape, composition, and efficiency of the neutron coincidence counter, but are also slightly affected by scattering, moderation, or neutron-induced fission within the sample being assayed. Typical values for most counter geometries are in the range of 30 to 100 μs. Thus the finite die-away time of the neutron coincidence counter causes the detection of prompt fission neutrons to be spread out over many microseconds. For large samples and typical counters, the mean lifetime may be comparable to, or longer than, the mean time interval between detected events.

As a result of the four effects described above, an actual observed pulse train may contain relatively few "real" coincident events among many "accidental" coincident events. Also, the real events will not stand out in any obvious way from the background of accidental events in the pulse train, as illustrated in train (b) in Figure 16.1. In order to visualize and quantify real and accidental events, it is helpful to use the interval distribution or the Rossi-alpha distribution.

16.2.2 The Interval Distribution

The interval distribution is the distribution of time intervals between detected events. This distribution is given by (Ref. 2):

$$I(t) = \exp\left[-\int_0^t Q(t)d(t)\right] \quad . \tag{16-4}$$

I(t) is the probability of detecting an interval of length t, and Q(t) is the probability of a second event as a function of time following a first event at $t = 0$. For a random neutron source the probability of a second event is constant in time. If the total count rate is T n/s, the normalized interval distribution is $I(t) = Te^{-Tt}$. In this case the interval distribution is exponential, and the most likely time for a following event to occur is immediately after the first event. On a semilogarithmic scale the interval distribution will be a straight line. If real coincidence events are present in addition to random events, the interval distribution is given by a more complex equation (Ref. 3). Figure 16.2 illustrates an interval distribution that contains both coincidence and random events.

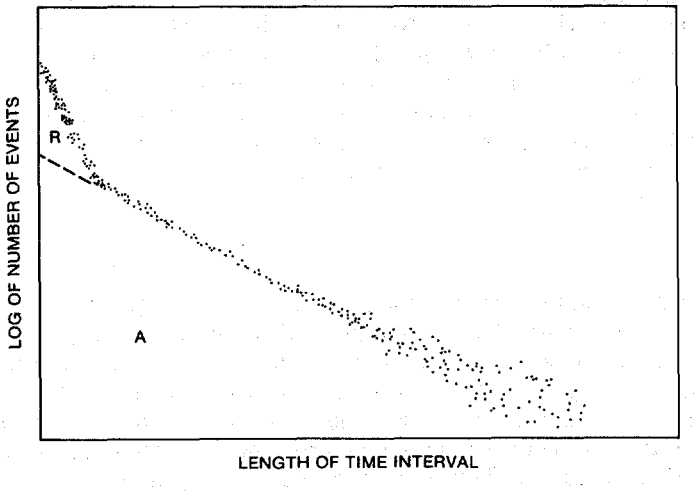

Fig. 16.2 *An interval distribution formed by real coincidence events R and accidental events A. The slope of the accidental distribution on this semilogarithmic scale is the total count rate T.*

16.2.3 The Rossi-Alpha Distribution

The Rossi-alpha distribution (Ref. 4), developed for reactor noise analysis, is another useful distribution. This distribution is obtained by starting a clock at t = 0 with the arrival of an arbitrary pulse. The clock continues to run, and each succeeding pulse is stored by a multiscaling circuit in a bin corresponding to its arrival time. A typical bin width might be 1 μs, and the total number of time bins available might range from 1024 to 4096. When the end of the total time interval is reached, the clock is stopped and the circuit remains idle until another event restarts the process at t = 0 again. Thus the Rossi-alpha distribution is the distribution in time of events that follow after an arbitrarily chosen starting event. If only random events are being detected, the distribution is constant with time. If real coincidence events are also present, the Rossi-alpha distribution is given by

$$S(t) = A + Re^{-t/\tau} \quad . \tag{16-5}$$

S(t) is the height of the distribution at time t; A is the accidental, or random, count rate; R is the real coincidence count rate; and τ is the detector die-away time. Figure 16.3 illustrates a Rossi-alpha distribution with R, A, and other variables (defined later) labeled. The exponential die-away of fission events is clearly seen in this distribution.

16.3 BASIC FEATURES OF COINCIDENCE CIRCUITS

16.3.1 Electronic Gates

Coincidence circuits often contain electronic components called "one-shots" or "gate generators" that produce an output pulse of fixed duration whenever an input pulse is received. Gate generators used to convert the input pulses from the neutron detector

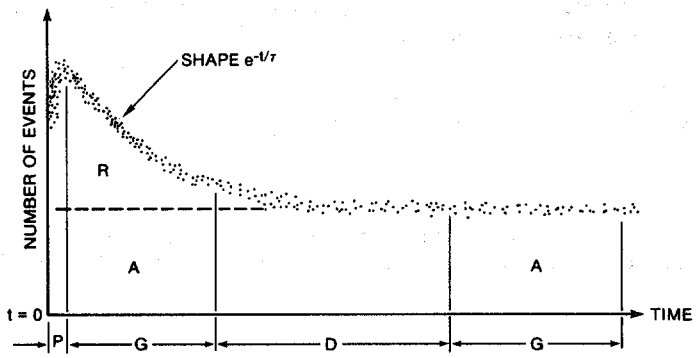

Fig. 16.3 *A Rossi-alpha distribution showing detected neutron events as a function of time following an arbitrary starting event. R represents real coincidence events, and A represents accidental coincidence events. P = predelay, G = prompt and delayed gates, D = long delay, and τ = die-away time.*

into very short output pulses are called "triggers." Gate generators used to convert the input pulses into long output pulses are called "gates." Such gate generators, as well as amplifiers, detectors, and other circuits, exhibit an electronic deadtime before they can function again. This deadtime is at least the length G of the gate. Depending on the design, this deadtime can be nonupdating or updating.

16.3.2 Updating and Nonupdating Deadtimes

A nonupdating, or nonparalyzable, deadtime is illustrated in pulse train (a) in Figure 16.4. Of the four events, events 1, 2, and 4 initiate gates, but event 3 does not and is lost. Using Equation 16-4, it can be shown that for a true random input rate T, the measured output rate T_m is

$$T_m = \frac{T}{1 + GT} \quad . \tag{16-6}$$

As the input rate becomes very large, the output rate will approach the limiting value 1/G, where G is the gate length.

An updating, or paralyzable, deadtime is illustrated in pulse train (b) in Figure 16.4. The appearance of event 3 causes the gate produced by event 2 to be extended or updated. Consequently, event 4 does not generate a new gate. Only events 1 and 2 initiate gates, and events 3 and 4 are lost. Using Equation 16-4, it can be shown that for random events

$$T_m = T e^{-GT} \quad . \tag{16-7}$$

As the input rate increases, the output rate increases up to a maximum value (which occurs when the input rate is 1/G) and then declines toward 0 (approaches paralysis) as the input rate continues to increase. For input rates that are small, identical deadtime corrections are obtained from Equations 16-6 and 16-7.

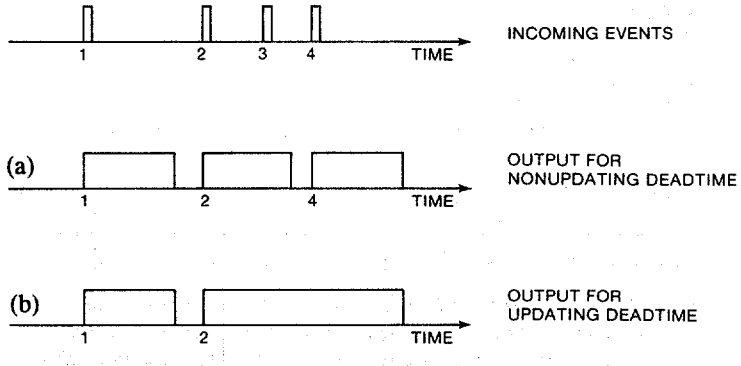

Fig. 16.4 *Two gate generators with different electronic deadtime characteristics: (a) nonupdating deadtime; (b) updating deadtime.*

16.3.3 Cross-Correlation and Autocorrelation Circuits

Electronic one-shots or gate generators can be combined with scalers in many possible ways to create coincidence circuits. Each combination will be subject to different electronic deadtimes and will require different equations for analysis. For neutron counting, cross-correlation or autocorrelation circuits are the most useful (Ref. 5). A simple cross-correlation measurement is shown in circuit (a) in Figure 16.5. Trigger pulses from detector 1 are compared with gates generated from detector 2. This type of circuit is most useful for very fast detector pulses and short gates because discrimination against detector noise is good and because very few accidental coincidences are produced.

Circuit (b) in Figure 16.5 illustrates an idealized autocorrelation measurement. Both detector inputs are first combined into one pulse train. Then every pulse in the train generates both a short trigger and a long gate, so that every pulse can be compared with every following pulse. Autocorrelation circuits are best suited for thermal-neutron counters because many detector banks can be summed together for high efficiency and because the substantial die-away time of the neutrons causes many overlaps between detector banks. Gate lengths are chosen to be comparable to the die-away time, and a separate, parallel circuit with a delayed trigger or gate is usually used for the subtraction of accidental coincidences (see Sections 16.4 and 16.5).

The autocorrelation circuits described in Section 16.4 and 16.5 are the most important circuits for neutron coincidence counting.

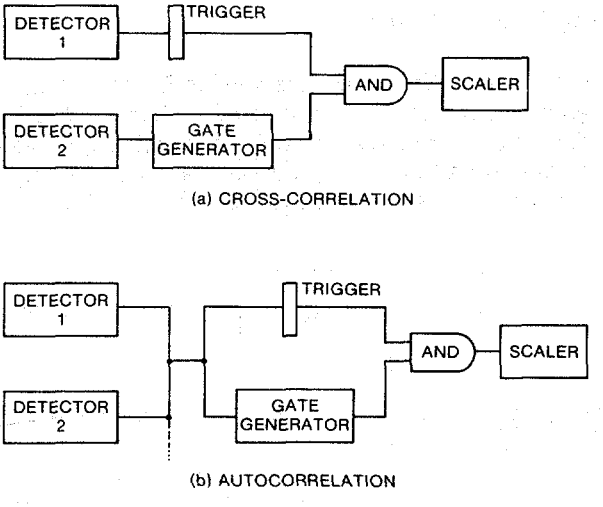

Fig. 16.5 *Two types of coincidence circuits: (a) cross-correlation; (b) autocorrelation.*

16.4 THREE COMMON COINCIDENCE CIRCUITS

16.4.1 Variable Deadtime Circuit

The variable deadtime circuit, or VDC, was developed in Europe for the assay of plutonium wastes (Refs. 6 through 8). It is a simple circuit (see Figure 16.6), but requires a complex analysis. The variable deadtime circuit consists of one short gate, typically 4 μs, that records most fission and accidental events, and one long gate, typically 32 to 128 μs, that misses most fission events but counts most accidental events. The difference between the two scalers is a measure of the rate of fissions. Both gates are nonupdating, so the net coincidence rate R, using Equation 16-6, is approximately given by

$$R \propto \frac{S_1}{1 - S_1G_1} - \frac{S_2}{1 - S_2G_2} \quad . \tag{16-8}$$

Here S_1 is the count rate in the scaler attached to the short gate, whose length is G_1, and S_2 is the count rate in the scaler attached to the long gate, whose length is G_2.

Equation 16-8 is useful only at count rates of several kilohertz or less because it does not treat the interference between fission and accidental events correctly. (More complex expressions are given in Refs. 9 and 10.) Additional difficulties arise when induced fissions in the sample cause longer fission chains (Refs. 11 and 12). For this reason the variable deadtime circuit is not practical for the assay of large, multiplying samples.

16.4.2 Updating One-Shot Circuit

An updating one-shot circuit (Ref. 10) is illustrated in Figure 16.7. The first half of the circuit generates prompt coincidences between a gate of length G and a short trigger. These coincidences consist of real coincidences (R) and accidental coincidences (A). In order to correct for these accidental events, it is necessary to add a long delay and then measure coincidences between a second, delayed gate of length G and the original short

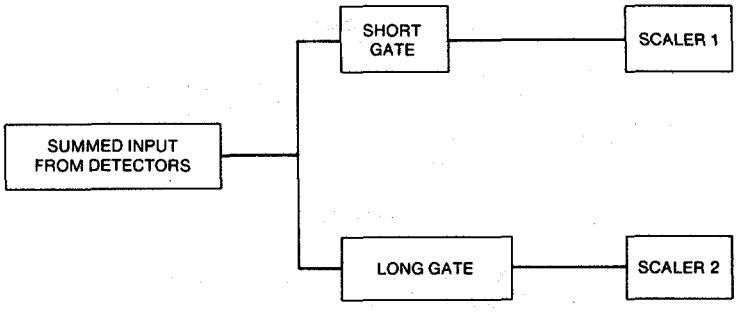

***Fig. 16.6** A variable deadtime circuit (VDC).*

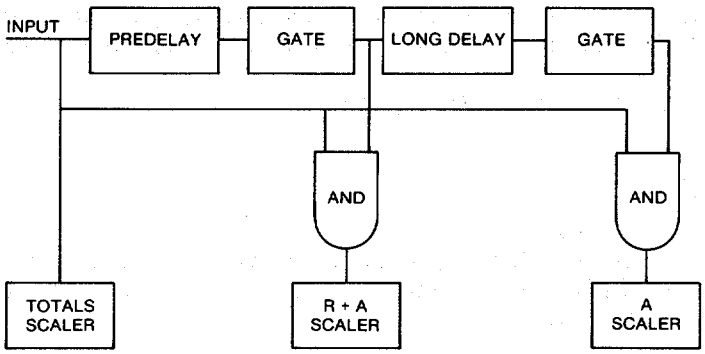

Fig. 16.7 *Updating one-shot circuit. The two one-shots are of equal length.*

trigger. If the long delay (D) is much longer than the mean neutron lifetime τ in the detector, the second coincidence circuit will measure only accidental events (A). The net coincidence response R is then given by the difference between the two scalers. Figure 16.3 illustrates this process.

Figure 16.3 also shows that an actual measurement of a Rossi-alpha distribution will be subject to several limitations: (a) pulse pileup and electronic deadtimes will perturb the distribution near $t = 0$, so it is customary to begin analysis at time P, the predelay; (b) because the distribution of real events extends beyond the gate interval G, some real coincidences are missed by the prompt gate; (c) in principle, some real events may appear in the delayed gate if D is not long enough. Taking these limitations into account, the true coincidence response of the updating one-shot circuit is given by

$$R = \frac{(R+A)\text{ scaler} - (A)\text{ scaler}}{e^{-P/\tau}(1-e^{-G/\tau})[1-e^{-(D+G)/\tau}]} e^{GT} \quad . \tag{16-9}$$

The exponential in the numerator, derived from Equation 16-7, is the correction for the triggers lost during the updating gate G. This large correction limits the usefulness of this circuit to count rates of 20 to 30 kHz or less. Nonupdating one-shot circuits have been built (Refs. 13 and 14), but they are also limited to low count rates.

16.4.3 Reduced Variance Logic

One interesting neutron coincidence circuit has its origins in the field of reactor noise analysis, which is the study of the fluctuations in the count rate of neutron detection systems. From these fluctuations it is possible to calculate the moments of the neutron count distribution (Feynman variance technique) (Ref. 4). The reduced variance logic (RVL) circuit applies this technique to the assay of nuclear material (Refs. 15 and 16).

The RVL circuit collects total neutron counts C over a short time interval of 100 to 2000 μs, depending on the application. This measurement is repeated for a large number of time intervals until a reasonable assay time of 100 to 1000 s is reached. From these measurements the circuit calculates the first moment C and the second moment $\overline{C^2}$ of

the count distribution. The variance-to-mean ratio of the count distribution is given by $(\overline{C^2} - \overline{C}^2)/\overline{C}$. For random counts that follow the Poisson distribution, this ratio is unity.

If correlated events are present, the parameter

$$Y = \frac{\overline{C^2} - \overline{C}^2}{\overline{C}} - 1 \qquad (16\text{-}10)$$

will be nonzero. This parameter is dependent on sample multiplication and independent of the spontaneous fission rate in the sample. Another combination of moments that is proportional to sample mass is

$$Q = \overline{C^2} - \overline{C}^2 - \overline{C} \quad . \qquad (16\text{-}11)$$

Q is independent of the random, uncorrelated background and is proportional to the coincidence count rate R.

The RVL circuit generates the parameters Q and Y for each sample assayed. For small, nonmultiplying samples, the effective ^{240}Pu mass of the sample is obtained from Q alone. For samples that exhibit significant self-multiplication, the ^{240}Pu mass is obtained indirectly from a nonlinear plot of Y as a function of $(Q/^{240}Pu_{eff})$ obtained with standards of known mass. A correction to Equation 16-11 for electronic deadtime at high count rates is given in Ref. 17.

In field applications, RVL circuits have been used to identify highly multiplying samples (Ref. 18). In fixed plant applications, a computer-based analysis system can be added to obtain higher moments of C and a time interval distribution of the counts. In principle, the RVL circuit uses the same count distribution and provides essentially the same assay information as the shift register circuit described in the following section. In practice, the RVL circuit in its present state of development requires more complex data interpretation algorithms and is limited to lower rates.

16.5 THE SHIFT REGISTER COINCIDENCE CIRCUIT

16.5.1 Principles of Shift Register Operation

In the preceding section it was noted that some common coincidence circuits require large corrections for electronic deadtime. Such corrections are required because coincidence analysis begins with one event at $t = 0$ and continues until $t = G$, the gate length. If n events arrive within a time G, the first event will start the gate and the other $n - 1$ will be detected. A second gate cannot be started until a time of length G has passed, thus creating a deadtime of that length.

An alternative approach is to store the incoming pulse train for a time G, so that every event can be compared with every other event for a time G. In effect, every pulse generates its own gate; it is not necessary for one gate to finish before the next can start. This storage of events eliminates the deadtime effect described above and allows operation at count rates of several hundred kilohertz or more.

It is possible to store incoming pulses for a time G by means of an integrated circuit called a shift register. The circuit consists of a series of clock-driven flip-flops linked together in stages. For example, a 64-stage shift register driven by a 2-MHz clock (0.5 μs/stage) defines a gate G of length 32 μs. Incoming pulses "shift" through the register one stage at a time and the whole process takes 32 μs.

This deadtime-free shift register concept was introduced by Boehnel (Ref. 5). Versions of the circuitry have been developed by Stephens, Swansen, and East (Ref. 19) and improved by Swansen (Refs. 20 and 21) and, most recently, by Lambert (Ref. 22). At present the shift register circuit is the most commonly used circuit for domestic and international coincidence counting applications. Examples are given in Chapter 17.

16.5.2 The R+A Gate

Operation of the shift register coincidence circuit is best visualized by referring to the Rossi-alpha distribution of Figure 16.3. This figure shows a prompt gate G that collects real and accidental coincidences (R+A) and a delayed gate G that collects only accidental coincidences (A). The two gates are separated by a long delay D. Note that coincidence counting does not begin until a short time interval P (the predelay) has passed. During this time, typically 3 to 6 μs, the Rossi-alpha distribution is perturbed by pulse pileup and electronic deadtimes in the amplifiers, and the true coincidence count rate cannot be measured. After the predelay, the prompt R+A gate is defined by a shift register that is typically 32 to 64 μs long.

A simplified diagram of a shift register circuit that measures R+A events is illustrated in Figure 16.8. The input (not illustrated) is the logical OR of all the amplifier-discriminator outputs, thus creating an autocorrelation circuit. Every input event, after the predelay P, passes into and through the shift register. Also, every event entering the shift register increments an up-down counter, and every event leaving the shift register decrements the up-down counter. Thus the up-down counter keeps a continuous record of the number of events in the shift register. Every input pulse, before it enters the

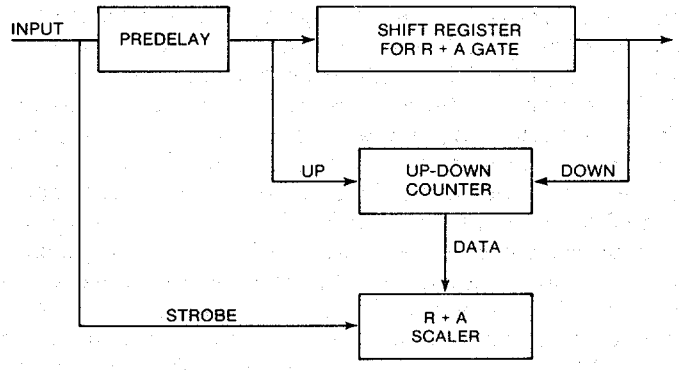

Fig. 16.8 *A simplified block diagram of a shift register coincidence circuit that measures real + accidental (R+A) events.*

predelay and the shift register, also causes the up-down counter to add its contents to the R+A scaler (strobe action).

The above sequence of events ensures that isolated, widely spaced events will never be registered in the R+A scaler. However, if two events appear with a time separation greater than P but less than P + G, then one event will be in the shift register (and the up-down counter will have a count of 1) when the other event strobes the contents of the up-down counter into the R+A scaler. Thus a coincidence will be recorded, as required by Figure 16.3. Note that if three or more events are present within the prescribed time interval, the counting algorithm will record all possible pairs of coincidences between events. For example,

For the following number of closely spaced events...	...the number of recorded coincidences will be	
0	0	
1	0	
2	1	
3	3	
4	6	
n	$n(n-1)/2$	(16-12)

The possible permutations in counting twofold coincidences can exceed the number of events. In practice this counting algorithm is neither beneficial nor harmful, but merely a consequence of treating all events equally.

The coincident events discussed above can represent two or more neutrons from one spontaneous fission (real fission event) or just the random overlap of background neutrons or neutrons from different fissions (accidental events). Thus the counts accumulated by the circuit described above are called R+A counts.

16.5.3 The A Gate

Real fission events R can be determined indirectly by adding a second complete shift register circuit that measures accidental events A. This circuit is identical to the R+A circuit except that a long delay D is introduced between the shift register that defines the A gate and the input event that strobes the contents of the up-down counter into the A scaler. The delay D is usually long compared to the detector die-away time so that no neutrons from fission events near $t = 0$ are still present, as illustrated in Figure 16.3. A common choice for D is approximately 1000 μs, which is very long compared to typical die-away times of 30 to 100 μs. When D is this long, the A scaler will record only accidental coincidences. These include random background events, uncorrelated overlaps between fission and background events, and uncorrelated overlaps between different fission events. The number of accidental events registered in the A scaler will be, within random counting fluctuations, the same as the number of accidental events registered in the R+A scaler if both the A and the R+A shift registers are exactly the same length in time. Then the net difference in counts received by the two scalers is the net real coincidence count R, which is proportional to the fission rate in the sample.

In practice the circuit that measures accidentals can be formed by introducing a second, delayed shift register circuit or by introducing a second, delayed strobe. The latter approach is used in recent circuit designs (Refs. 20 through 22) for simplicity and because it is easy to produce A and R+A gates of the same length. Figure 16.9 (Ref. 23) is a block diagram of a recent shift register coincidence circuit design that includes totals (T), R+A, and A scalers.

The A scaler records accidental coincidences between the total neutron events recorded, and the following relationship is true within random counting fluctuations:

$$A = G T^2 \quad , \tag{16-13}$$

where A and T are expressed as count rates, and G is the coincidence gate length (Ref. 24). This nonlinear relationship shows that A will exceed T when the total count rate is greater than 1/G. By means of Equation 16-13 it is possible to calculate A rather than measure it. However, it is better to measure A with the circuit described above because this corrects continuously and automatically for any change in the total neutron count rate during the assay. Equation 16-13 can then be used later as a diagnostic check for count-rate variations or instrument performance.

16.5.4 Net Coincidence Response R

From Figure 16.3 and the above discussion the true shift register coincidence response is related to the measured scaler outputs by the equation

$$R = \frac{(R+A)\text{ scaler} - (A)\text{ scaler}}{e^{-P/\tau}(1 - e^{-G/\tau})[1 - e^{-(D+G)/\tau}]} \quad . \tag{16-14}$$

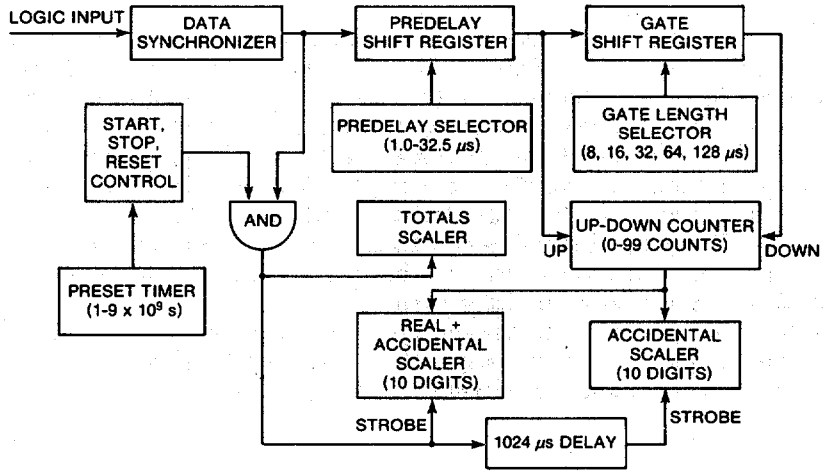

***Fig. 16.9** Block diagram of a complete shift register coincidence circuit including totals, R+A, and A scalers (Ref. 23).*

Equation 16-14 is identical to Equation 16-9 except that the large exponential deadtime correction is not required for the shift register. Smaller corrections for amplifier deadtimes are given in Section 16.6 below. The term $[1 - e^{-(D+G)/\tau}]$ should be very close to unity if the delay D is much longer than the detector die-away time τ. Consequently, this term will be dropped in the following discussions.

In Equation 16-14, R represents the total number of coincidence counts that could be obtained if finite predelays, gate lengths, or delays were not required. In practice it is customary to keep P, G, and D fixed and allow for their effects in the process of calibration with known standards. Then R = (R+A) scaler − (A) scaler is considered to be the true, observed coincidence response. An important equation that relates R to the physical properties of the sample, the detector, and the coincidence circuit can be derived from Equations 16-2, 16-12, and 16-14 (Refs. 5 and 25):

$$R = m_{240}\,(473 \text{ fissions/s-g})\varepsilon^2 e^{-P/\tau}\,(1 - e^{-G/\tau}) \sum_{\nu} P(\nu)\,\frac{\nu(\nu - 1)}{2!} \tag{16-15}$$

where

R = true coincidence count rate
m_{240} = ^{240}Pu-effective mass of the sample
ε = absolute detector efficiency
ν = spontaneous fission neutron multiplicity
$P(\nu)$ = multiplicity distribution
P = predelay
G = coincidence gate length
τ = detector die-away time.

Equation 16-15 illustrates again that the response of the shift register circuit to ν closely spaced events is proportional to $\nu(\nu - 1)/2$, whereas the response of a conventional circuit would be proportional to $(\nu - 1)$. For practical values of ε and ν, the differences are not great and are automatically accounted for in the calibration process. In Section 16.5.2 it was shown that the expression $\nu(\nu - 1)/2$ represents the sum of all twofold coincidences for ν closely spaced events. Thus the shift register collects all possible valid coincidences. The response of the circuit is still linear with respect to sample mass. However, the sample self-multiplication effects described in Section 16.8 below do affect shift register circuits more than conventional circuits, so that the shift register circuits require larger correction factors.

Equation 16-15 provides a means of determining the detector die-away time τ. If the same sample is assayed in the same way at two different gate settings G_1 and G_2, where G_2 is twice G_1, with the coincidence results R_1 and R_2, respectively, then

$$\tau = -G_1/\ln\,(R_2/R_1 - 1) \quad . \tag{16-16}$$

16.6 DEADTIME CORRECTIONS FOR THE SHIFT REGISTER

In the preceding section it was shown that the coincidence gate length G does not introduce deadtimes into the shift register circuit, which permits operation at count rates above 100 kHz. At such high rates, however, a number of smaller deadtimes associated with the analog and digital parts of the circuitry become apparent. These include

- detector charge collection time
- amplifier pulse-shaping time
- amplifier baseline restoration time
- losses in the discriminator OR gate
- shift register input synchronization losses.

These deadtime effects can be studied with time-correlated californium neutron sources, with uncorrelated AmLi neutron sources, and with new digital random pulsers (Ref. 26). Even though the deadtimes can often be studied singly or together, the total effect is difficult to understand exactly because each deadtime perturbs the pulse train and alters the effect of the deadtimes that follow. This section summarizes what is presently known about these deadtimes. Overall empirical correction factors are given, and several electronic improvements that reduce deadtime are described.

16.6.1 Detector and Amplifier Deadtimes

For most shift register systems in use today, the analog electronic components consist of (a) gas-filled proportional counters, (b) charge-sensitive preamplifiers, (c) amplifiers, and (d) discriminators. As described in Section 13.2, a charge signal can be obtained from the gas counter within an average time of 1 to 2 μs after the neutron interaction. This time dispersion is limited by variations in the spatial position of the interaction site, and is not actually a deadtime. However, the ability of the detector to resolve two separate pulses will be comparable to the time dispersion. The preamplifier output pulse has a risetime of about 0.1 μs, and the amplifier time constant is usually 0.15 or 0.5 μs. If all of the electrical components listed above are linked so that one preamplifier and one amplifier with 0.5-μs time constant serve seven gas counters, a total deadtime of about 5 μs is observed (Ref. 27). In practice this deadtime is reduced by using multiple preamplifier-amplifier chains, as described in Section 16.6.4.

The amplifier output enters a discriminator that consists of a level detector and a short one-shot. The one-shot output is 50 to 150 ns long.

16.6.2 Bias Resulting from Pulse Pileup

In addition to actual deadtimes, the electrical components can produce a bias in the shift register output. Bias is defined as the difference between the R+A and A counting rates when a random source such as AmLi is used. For a random source the difference (R+A) − A should be zero; if it is not, the percent bias is 100 R/A. Possible sources of bias include electronic noise; uncompensated amplifier pole zero; shift register input

capacitance; a deadtime longer than the predelay P; or amplifier baseline displacement following a pulse, which is the most important source of bias if the electronic components are properly adjusted to minimize the other sources. Any closely following pulses that fall on the displaced baseline before it is fully restored to zero have a different probability of triggering the discriminator. Bias resulting from pulse pileup is proportional to the square of the count rate and may become noticeable at high count rates. If the baseline is not fully restored in a time less than the predelay time, the effect will extend into the R+A gate and a bias will result.

Figure 16.10 (Ref. 28) illustrates a bias measurement as a function of predelay. The measurement used a coincidence counter with six amplifier channels. The observed bias was reduced to an acceptable value of 0.01% or less for predelay settings of 4.5 μs or more. These results are typical for well-adjusted electronics. For some high-efficiency and long die-away-time counters that operate at rates above 100 kHz, a conservative predelay setting of 6 to 8 μs may be warranted, but in general 4.5 μs is sufficient. At high count rates, R is typically on the order of 1% of A; a pulse pileup bias of 0.01% in R/A implies a relative bias of 1% in R, a bias that is only barely acceptable.

16.6.3 Digital Deadtimes

Because of the deadtime in the amplifier-discriminator chain, it is customary to divide the detector outputs of a coincidence counter among four to six amplifiers. Each amplifier channel may serve three to seven detectors. The discriminator outputs of each channel are then "ORed" together before they enter the shift register (autocorrelation mode). Now the deadtime after the OR gate is much less than before provided the two

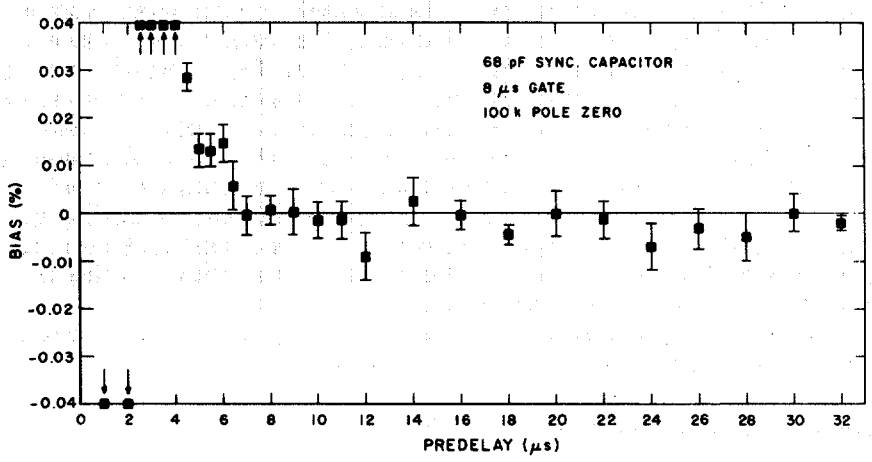

Fig. 16.10 *Shift register coincidence bias R/A as a function of predelay P for electronics with 0.5 μs time constant, as measured with a strong random AmLi neutron source. For this measurement, bias was minimized by using optimum values of 100 kΩ for the amplifier pole-zero resistance and 68 pF for the shift register input synchronizer capacitor. Sensitivity to any remaining bias was maximized by using an 8-μs coincidence gate G for the measurements (Ref. 28).*

events are from different channels. The deadtime contribution of the OR gate itself can be calculated under the assumptions that (a) no losses occur within a channel because of the longer preceding amplifier deadtime and (b) losses between channels are due to pulse overlap.

$$\text{OR gate overlap rate} = \frac{n(n-1)}{2!}2(\text{disc. output width})(T/n)^2, \tag{16-17}$$

where n is the number of channels and T is the total count rate. The ideal deadtime for an OR gate accepting 50-ns-wide pulses is then

$$\text{OR gate deadtime} = \frac{n-1}{n}(50\text{ ns}) \quad . \tag{16-18}$$

This deadtime is for total events; the coincidence deadtime has not been calculated but would be larger.

The output of the OR gate is a digital pulse stream that enters the shift register. At this point the 50-ns-wide pulses must be synchronized with the 500-ns-wide shift register stages. The limit of one pulse per stage means that some closely following pulses will be lost unless a derandomizing buffer (Section 16.6.5) is used. These losses have been measured with a digital random pulser, as illustrated in Figure 16.11. The shape of this curve is given by

$$\text{measured totals} = (1 - e^{-pT})/p \tag{16-19}$$

where p is the shift register clock period (500 ns in this case) and T is the total input rate (Ref. 29). At low rates, Equation 16-19 yields a nonupdating deadtime of p/2; at high

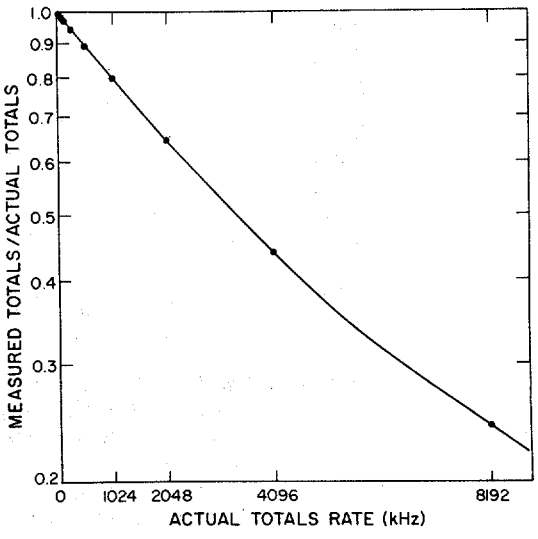

Fig. 16.11 *Shift register synchronizer deadtime as measured with a digital random pulser attached directly to the synchronizer input. The shift register clock period is 500 ns and the digital random pulser has a pulse-pair resolution of 60 ns.*

rates, the deadtime approaches p. The coincidence deadtime is on the order of 2p, as described in Ref. 29. In general, the synchronizer deadtime is small compared to the amplifier deadtime, but it can be appreciable at high count rates. For example, at 256 kHz the totals losses will be 6% and the corresponding coincidence losses will be larger.

16.6.4 Empirical Deadtime Correction Formulas

The total effect of the analog and digital deadtimes described above has not been calculated, but can be determined empirically with californium and AmLi neutron sources. The coincidence deadtime δ_c can be determined by placing a californium source in a fixed location inside a well counter and measuring the coincidence response as stronger and stronger AmLi sources are introduced. During these measurements it is important (1) to center the sources so that all detector channels observe equal count rates and (2) to keep the sources well separated so that scattering effects are minimized. The result of such a measurement is shown in Figure 16.12. Within measurement uncertainties the overall coincidence deadtime is well represented by the updating deadtime equation (Equation 16-7). The totals deadtime δ_t can be measured by the source addition technique, where two californium or AmLi sources are measured in the counter, first separately and then together. An updating deadtime equation also works well for the total count rate correction. Bias can be measured by placing only random AmLi sources in the counter.

Under the assumption that the electronic components have been adjusted so that bias is negligible, as discussed in Section 16.6.2, the overall empirical deadtime correction equations are

$$T(\text{corrected}) = T_m e^{\delta_t T_m} \tag{16-20}$$

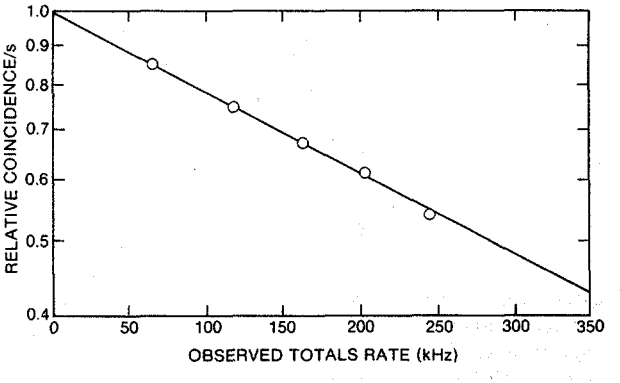

Fig. 16.12 Semilogarithmic plot of relative coincidence response from a californium source as a function of increasing totals count rate resulting from additional AmLi sources. The points are measured values; the line is a least-squares fit to an exponential with deadtime coefficient δ_c = 2.4 μs (Ref. 24).

$$R(\text{corrected}) = R_m e^{\delta_c T_m} \tag{16-21}$$

where T_m is the measured totals rate and R_m is the measured coincidence rate, (R+A) scaler − (A) scaler. Note that in Equations 16-20 and 16-21 the argument of the exponential contains T_m instead of the corrected rate T that appears in Equation 16-7. The use of T_m is a convenient approximation at rates up to about 100 kHz, but at higher rates this approximation forces δ_t and δ_c to become functions of the count rate rather than constants. Values of δ_t and δ_c appropriate for the amplifier chains and 2-MHz-clock shift registers most commonly used today are summarized in Table 16-1 (data compiled from Refs. 27, 30, and 31). For example, six channels of 0.15-μs time-constant amplifiers will have $\delta_c = 0.62$ μs and will exhibit an overall coincidence deadtime of about 6% at 100-kHz counting rates.

From Table 16-1 it is apparent that the deadtime coefficient depends weakly on the detector gas mixture and strongly on the number of amplifier channels available. The number of detector tubes per amplifier channel has no measurable effect on the coefficients, although this situation may change if the detector tubes are subject to count rates in excess of about 20 kHz per tube. Note that all of the coincidence deadtime coefficients in Table 16-1 were measured with a californium source ($\nu = 3.757$) whereas the isotope usually assayed is ^{240}Pu ($\nu = 2.16$). The effect of this difference is not yet known.

16.6.5 AMPTEK Electronics and Derandomizing Buffer

Recent improvements in the analog and digital electronics include faster amplifiers, shorter discriminator outputs, and a derandomizing buffer at the shift register input (Ref. 31). The faster amplifier, which has an effective time constant of about 0.15 μs, consists of a Model A-111 hybrid charge-sensitive preamplifier, discriminator, and pulse shaper manufactured by AMPTEK, Inc., of Bedford, Massachusetts. This unit provides sufficient gain and signal/noise ratio if the ^3He detector tubes are operated at +1700 V.

Table 16-1. Compilation of empirical deadtime coefficients for shift-register-based coincidence counters (Refs. 27, 30, 31)

^3He Detector Gas Additive	Number of Detectors/ Channel	Number of Amplifier Channels	Amplifier Time Constant (μs)	Deadtime (μs)		
				Totals, δ_t	Coincidence, δ_c 0-100 kHz	Coincidence, δ_c 0-500 kHz
$Ar + CH_4$	7	6	0.5[a]	0.6	2.4	$2.3 + 1.6 \times 10^{-6} T_m$
$Ar + CH_4$	7	4	0.5	0.87	3.0	$2.8 + 2.7 \times 10^{-6} T_m$
$Ar + CH_4$	7	2	0.5	2.9	4.7	
$Ar + CH_4$	7	1	0.5	4.9	12.6	
5% CO_2	7	6	0.5	0.9	3.1	
$Ar + CH_4$	3	6	0.15[b]	0.16	0.62	$0.62 + 0.20 \times 10^{-6} T_m$

[a]Los Alamos-designed 0.5-μs time-constant amplifier chain (Refs. 22, 23).

[b]AMPTEK A-111 integrated circuit with approximately 0.15-μs time constant in conjunction with a derandomizing buffer on the shift register input (see Section 16.6.5).

The Model A-111 has been incorporated with other electronics on a printed circuit board mounted in a small shielded enclosure. Each enclosure contains an amplifier insensitive to external noise, an LED output monitor, a discriminator output shortened to 50 ns, and connections for "ORing" multiple channels together. Six channels of A-111 units can be operated with a reduced predelay of 3 μs with less than 0.01% bias.

The derandomizing buffer holds pulses that are waiting to enter the shift register, thus eliminating the input synchronization losses described in Section 16.6.3. Input pulses separated by less than 0.5 μs—the shift register clock period—are stored in a 16-count buffer until the shift register can accept them. This circuit eliminates the coincidence deadtime of roughly 1.0 μs associated with the shift register input and permits counting at rates approaching 2 MHz with virtually no synchronizer counting losses. However, as the derandomizing buffer stretches pulse strings out in time, it may create strings longer than the predelay and thereby produce a bias. Because the AMPTEK A-111 amplifier requires a predelay of only 3 μs, the maximum recommended totals rate for less than 0.01% bias is 500 kHz.

With the AMPTEK electronics and the derandomizing buffer, the coincidence deadtime is reduced by a factor of 4 to about 0.6 μs, as noted in Table 16-1. This combination permits passive assays of almost any plutonium samples, with criticality safety of the sample in the well being the only limit.

16.7 UNCERTAINTIES RESULTING FROM COUNTING STATISTICS

In principle the effect of counting statistics on the coincidence response is very complex because the input pulse train contains both random and correlated events and because correlated events can overlap in many ways. Some of the complicating factors are described briefly in this section. For practical coincidence counters these factors are not large, and it is usually possible to calculate measurement uncertainties for coincidence counting with the simple Equation 16-23 given in Section 16.7.1 below.

The major factor that complicates measurement uncertainties is the nonrandom distribution of neutrons from spontaneous fission. Random neutrons from background or (α,n) events follow a Poisson distribution: for n counts, the variance is n and the relative error is $\sigma_n/n = \sqrt{\text{var}(n)}/n = 1/\sqrt{n}$. However, if a spontaneous fission source emits a total of T neutrons in S fissions, with $T = \bar{\nu}S$ where $\bar{\nu}$ is the mean fission multiplicity, the relative error is $1/\sqrt{S}$ rather than $1/\sqrt{T}$. The number of spontaneous fissions follows a Poisson distribution, but the total number of neutrons does not. This is because the emission of more than one neutron per fission does not provide any more information to reduce the measurement uncertainty.

Boehnel (Ref. 5) has shown that counting n spontaneous fission neutrons with an efficiency ε has a variance

$$\frac{\text{var}(n)}{n} = 1 + \varepsilon \frac{\overline{\nu^2} - \bar{\nu}}{\bar{\nu}} \quad . \tag{16-22}$$

If $\bar{\nu}$ approaches 1 or ε approaches 0, the variance approaches the Poisson distribution value of var(n) = n, but always remains larger. Equation 16-22 implies that the

measurement uncertainty will depend on the multiplicity of the fission source, the fraction of random events ($\nu = 1$) present, and the detector efficiency. Other complicating factors are the detector die-away time and the total count rate, which affect the degree to which events overlap. Coincidence counting will then introduce additional complications.

16.7.1 Simple Error Equation for the Shift Register

For practical values of n and ε, the deviations from the Poisson distribution are not large, as suggested by Equation 16-22 and pulse train (b) in Figure 16.1. If the (R+A) and (A) registers are assumed to be uncorrelated and to follow the Poisson distribution, the relative error is

$$\frac{\sigma R}{R} = \frac{\sqrt{(R+A) + A}}{R} = \frac{\sqrt{R + 2A}}{R} \quad . \tag{16-23}$$

This approximation has been compared with a wide variety of actual measurements and is usually correct to within 15% for plutonium oxide and 25% for californium. Since other uncertainties often limit assay accuracy, it is usually sufficient to know the statistical uncertainty to this level. More exact equations are given in Ref. 5.

Using Equation 16-13, the above uncertainty equation can be rewritten as

$$\frac{\sigma R}{R} = \frac{\sqrt{R + 2GT^2}}{R\sqrt{t}} \tag{16-24}$$

where R and T are deadtime-corrected count rates (Equations 16-20 and 16-21), and t is the count time. In this form, Equation 16-24 is valid for the variable deadtime and updating one-shot circuits as well as for the shift register, as confirmed by measurement (Ref. 10).

Since R is proportional to $(1 - e^{-G/\tau})$, the optimum value of gate length G that minimizes the relative error for a given die-away time τ can be derived by differentiating Equation 16-24. The result is

$$G = \tau(e^{G/\tau} - 1)/2 \approx 1.257\tau \quad . \tag{16-25}$$

16.7.2 Uncertainties for Passive and Active Counting

In passive neutron coincidence counting, the measured total response is proportional to $\varepsilon m_{240} t$, and the measured coincidence response is proportional to $\varepsilon^2 m_{240} t$, where m_{240} is the ^{240}Pu-effective mass and t is the count time. The statistical measurement uncertainty (Equation 16-23 or 16-24) is then proportional to

$$\frac{\sigma R}{R} \propto \frac{\sqrt{k_1 m_{240} + 2k_2 G m_{240}^2}}{\varepsilon m_{240}\sqrt{t}} \tag{16-26}$$

where k_1 and k_2 are two constants of proportionality. For very small samples the relative error is proportional to $1/\sqrt{m_{240}}$; for large samples the relative error is independent of sample mass. In either case the relative error is proportional to $1/\varepsilon$, which implies that the efficiency of the passive well counter should be as high as possible.

Active assay of uranium samples can be carried out with the Active Well Coincidence Counter (AWCC), which uses AmLi sources to induce fissions in ^{235}U (see Section 17.3.1). For the AWCC the statistical measurement uncertainty is again given by Equation 16-23 or 16-24. The coincidence response is proportional to $\varepsilon^2 m_{235} t S$, where m_{235} is the ^{235}U mass, t is the count time, and S is the AmLi source strength. Although the totals response is increased by these induced fissions, the effect is small in practice and for error calculations it is reasonable to assume that the totals response is directly proportional to εSt. Then

$$\frac{\sigma R}{R} \propto \frac{\sqrt{k_1 m_{235} S + 2Gk_2 S^2}}{\varepsilon m_{235} S \sqrt{t}} \tag{16-27}$$

where k_1 and k_2 are two constants of proportionality. For large uranium masses and weak sources, the relative error is proportional to $1/\sqrt{m_{235}S}$, as expected. For strong sources, the relative error is proportional to $1/\varepsilon m_{235}$.

This last relationship has several interesting consequences. First, the relative error is independent of source strength for sources large enough to ensure that R is much less than A. This feature has the advantage that the sources need only be large enough to meet this criterion, which in practice has been measured as 2×10^4 n/s (for two sources, negligible background, and no passive signal from the sample)(Ref. 32). However, this feature has the disadvantage that assay precision cannot be improved by introducing larger sources. Once G, ε, k_1, and k_2 are determined by the design of the well counter, the assay precision can only be varied by varying the counting time. Second, the absolute assay precision is almost independent of sample mass and is determined primarily by the accidental coincidence rate. For the AWCC described in Ref. 32, the absolute assay precision in the "fast configuration" for 1000-s count times is equivalent to 18 g of ^{235}U.

16.8 EFFECTS OF SAMPLE SELF-MULTIPLICATION

Among the effects that may perturb passive coincidence counting, self-multiplication of the coincidence response resulting from induced fissions within the sample is usually dominant. This self-multiplication takes place in all plutonium samples and (to a lesser extent) in all uranium samples. Passive coincidence counters respond to induced fissions as well as to spontaneous fissions. Thus the response from a given amount of spontaneously fissioning material is multiplied and appears to indicate more nuclear material than is actually present. This section describes the magnitude of this effect for plutonium and provides a self-multiplication correction factor that is useful for some assay situations.

16.8.1 Origin of Self-Multiplication Effects

There are two common internal sources of neutrons that induce fissions. One source is the spontaneously fissioning isotopes themselves. For example, neutrons emitted by ^{240}Pu may be captured by ^{239}Pu nuclei and induce these nuclei to fission. The spontaneous fission multiplicity $\nu_s = 2.16$, and the thermal-neutron-induced fission multiplicity $\nu_I = 2.88$ (from Table 11-1). The coincidence circuitry cannot in practice distinguish between these two multiplicities so that both types of fissions may be detected.

The other common source of neutrons is from (α,n) reactions with low-Z elements in the matrix. For example, in plutonium oxide, alpha particles from ^{238}Pu may react with ^{17}O or ^{18}O to create additional neutrons that may induce fissions in ^{239}Pu. The (α,n) neutrons, with multiplicity 1, do not in themselves produce a coincidence response; however, the induced fission neutrons, with multiplicity $\nu_I = 2.88$, do. The magnitude of this coincidence response depends on the alpha emitter source strength, the low-Z element density, the degree of mixing between alpha emitters and low-Z elements, the fissile isotope density, and the geometry of the sample, and in general is not proportional to the quantity of the spontaneously fissioning isotopes that are to be assayed.

The multiplication of internal neutron sources by induced fission is the same process that eventually leads to criticality. What is surprising is the appearance of multiplication effects in the assay of relatively small samples whose mass is far from critical. Even 10-g samples of plutonium metal show 5% enhancements in the coincidence response. At 4000 g of plutonium metal, not too far from criticality, the multiplication of the total neutron output is roughly a factor of 2 and the multiplication of the coincidence response is roughly a factor of 10.

The magnitude of self-multiplication effects on the passive coincidence assay of PuO_2 cans is illustrated in Figure 16.13 (Ref. 33). The data show a definite upward curvature, and the deviation from a straight line determined by the smallest samples amounts to about 38% at the largest sample, 779 g of PuO_2. In the past, self-multiplication effects have often been masked by presenting data without electronic deadtime corrections or by drawing a straight line that seems to pass through most of the data even though the slope does not fit the smallest samples. The latter error is most easily avoided by tabulating coincidence response per gram, as in column 3 of Table 16-2. The following sections discuss other features of Table 16-2 that describe self-multiplication corrections applied to the data.

16.8.2 Calculational Results

Self-multiplication within a sample can be calculated by Monte Carlo techniques. The results of calculations done for the samples listed in Table 16-2 are given in columns 5 to 9. These calculations were carried out with the Monte Carlo code described in Ref. 33; however, the detector itself was not modeled in detail since it was necessary to obtain only the net leakage multiplication across a surface surrounding the sample. The Monte Carlo code selected initial (α,n) or spontaneous fission neutrons according to the ratio

$$\alpha = N_\alpha/\nu_s N_s \tag{16-28}$$

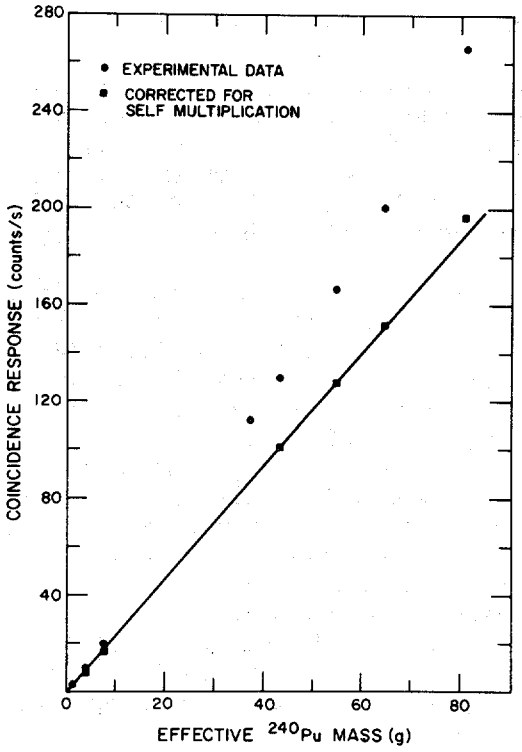

Fig. 16.13 *Coincidence response of PuO_2 standards. The upward curvature in the data is due to self-multiplication in PuO_2. Monte Carlo calculations described in the text were carried out for all but the first and fourth samples in order to correct for self-multiplication, yielding a linear fit to the data.*

where N_α is the number of (α,n) reactions and N_s is the number of spontaneous fissions. The values for α, obtained from Equation 16-32 or 16-35, are given in column 4 of Table 16-2. Each neutron-induced fission chain was followed to its end. The Monte Carlo code calculated the leakage multiplication M_L (defined in Chapter 14), which is related to the probability of fission p by the relation

$$M_L = \frac{1 - p}{1 - p\,\nu_I} \quad . \tag{16-29}$$

The calculated values of M_L are given in column 5 of Table 16-2. These are the ratios by which the total neutron count is enhanced by multiplication, with leakage, absorption, fission, and reflection taken into account. For simplicity, the leakage multiplication is denoted by M in the remaining discussion.

Table 16-2. Self-multiplication correction factors for the plutonium oxide samples in Figure 16.13. Columns 5 through 9 are based on Monte Carlo calculations, and columns 10 and 11 are based on the R/T ratio

1	2	3	4	5	6	7	8	9	10	11
Sample Mass (g)	^{240}Pu-Effective (%)	Coincidence Response/ g-s	α	Leakage Mult., M_L	f_{sf}	$f_{\alpha n}$	Correction Factor, CF	Corrected Response/ g-s	From R/T ratio	
									M_L	CF
20	6.0	2.35(2)	0.66				1.02(1)	2.31(3)		
60	6.4	2.42(2)	1.43	1.005	0.024	0.020	1.04(1)	2.32(3)	1.003	1.03
120	6.4	2.53(2)	1.36	1.010	0.049	0.035	1.08(1)	2.33(3)	1.012	1.08
480	7.8	2.99(3)	0.74				1.28(1)	2.34(4)	1.044	1.26
459	9.5	2.98(3)	0.64	1.046	0.192	0.068	1.26(1)	2.36(4)	1.048	1.28
556	9.9	3.03(3)	0.62	1.049	0.215	0.075	1.29(1)	2.35(4)	1.043	1.25
615	10.6	3.08(3)	0.60	1.056	0.260	0.084	1.34(1)	2.30(4)	1.052	1.30
779	10.4	3.26(3)	0.61	1.061	0.285	0.095	1.38(1)	2.36(4)	1.070	1.41

The Monte Carlo code also calculated a coincidence correction factor

$$CF = 1 + f_{sf} + f_{\alpha n} \tag{16-30}$$

where $1 + f_{sf}$ is the coincidence correction for net multiplication of spontaneous fission neutrons, and $f_{\alpha n}$ is the additional correction for net multiplication of (α,n) neutrons. In Table 16-2, columns 6 and 7 show the relative size of these two induced-fission multiplication effects for the plutonium oxide samples measured. Column 8 shows the overall correction factor CF, and column 9 demonstrates that the corrected coincidence response per gram is now nearly constant.

With the code described above, a series of reference calculations were made to determine the effect of sample mass, density, isotopic composition, and water content on the coincidence correction factor. The results are plotted in Figure 16-14 (Ref. 33). All calculations represent variations about an arbitrary nominal sample of 800-g PuO_2, with a density of 1.3 g oxide/cm^3. This sample contains 706 g of plutonium at 10% $^{240}Pu_{eff}$ and 1 wt% water, in an 8.35-cm-i.d. container. For each calculation, only one parameter was varied from the nominal values. For the mass and density variations, the fill height was adjusted to conserve mass. For the H_2O content variation, the sample density was

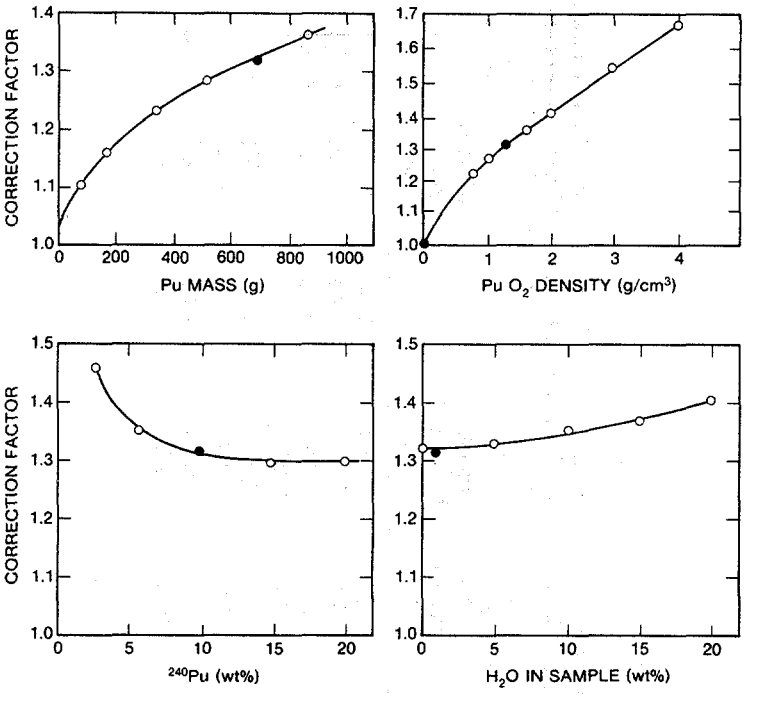

Fig. 16.14 *Monte Carlo calculations of self-multiplication effects of various parameters on coincidence counting of PuO_2. The solid data points denote the nominal calculation.*

adjusted to conserve volume. Figure 16.14 shows that coincidence correction factors are appreciable even at low mass and low density.

The curves in Figure 16.14 can be used to estimate coincidence correction factors for other similar plutonium oxide samples. The exact range of applicability is not known. For the samples in Table 16-2, the correction factors were calculated directly by the Monte Carlo code, except for the first and fourth samples, which were extrapolated from Figure 16.14, with consistent results.

16.8.3 Effects on Shift Register Response

It is possible to write expressions for the effects of sample self-multiplication on the shift register response. The total neutron count rate T, after subtraction of the background count rate b, is given by

$$T - b = m_{240}\,(473/\text{s-g})\,\varepsilon\, M\nu_s(1 + \alpha) \tag{16-31}$$

where m_{240} is the effective ^{240}Pu mass, ε is the detector efficiency, M is the leakage multiplication, ν_s is the spontaneous fission multiplicity, and α is defined by Equation 16-28. If all other quantities are known, α can be determined by inverting Equation 16-31:

$$1 + \alpha = (T - b)/m_{240}(473/\text{s-g})\varepsilon\, M\, \nu_s \quad . \tag{16-32}$$

The coincidence count rate R is given by the following equations (Ref. 34):

$$R = m_{240}\,(473/\text{s-g})\,\varepsilon^2\,\frac{\overline{\nu(\nu - 1)}}{2}\,F \quad , \tag{16-33}$$

$$\overline{\nu(\nu - 1)} = M^2\left[\frac{\overline{\nu_s(\nu_s - 1)}}{1 + \alpha\,\nu_s} + \frac{(M - 1)}{\nu_I - 1}\,\frac{(1 + \alpha)}{1 + \alpha\,\nu_s}\,\nu_s\,\overline{\nu_I(\nu_I - 1)}\right] \quad , \tag{16-34}$$

where $\overline{\nu_s(\nu_s - 1)}$ and $\overline{\nu_I(\nu_I - 1)}$ are the reduced second moments of the spontaneous and induced fission multiplicity distributions.

Equation 16-33 is similar to Equation 16-15, with F representing the fraction of coincidences measured, $e^{-P/\tau}(1 - e^{-G/\tau})$. These equations assume that all fission chains produced from the original fission appear to be simultaneous within the resolving time of the coincidence counter. This assumption, called the "superfission concept" (Ref. 5), is valid for thermal-neutron counters because of their long die-away time.

From Equations 16-31 and 16-33 for T and R, and from columns 5 and 8 of Table 16-2, it is apparent that sample self-multiplication affects coincidence counting more than totals counting. As a simple example of this effect, suppose that a spontaneous fission releases two neutrons, one of which is captured by a fissile nucleus which in turn releases three neutrons upon fissioning. The total number of neutrons has increased

from two to four (M = 2). However, the coincidence response has increased from one to six (CF = 6). Thus the ratio R/T has increased with multiplication. Laboratory measurements have shown that R/T can be used as a measure of multiplication. This ratio is the basis of the simple self-multiplication correction described in the following section.

16.8.4 A Simple Correction Factor for Self-Multiplication

Since it is usually not possible to perform a Monte Carlo calculation to determine the self-multiplication of each sample to be assayed, there is a strong need for a self-multiplication correction that can be determined for each sample from the measured parameters R and T. As mentioned earlier, the ratio R/T is sensitive to sample multiplication so that it is possible to use R for the assay and R/T for a multiplication correction. The procedure for calculating this correction for plutonium samples follows.

Step 1: Assay a small 10- or 20-g reference sample that, as an approximation, can be considered as nonmultiplying. Use the same physical configuration and electronic settings as those to be used in Step 2 for assay of larger samples. This measurement yields the values R_0, T_0, and α_0. If the nonmultiplying sample is pure metal, $\alpha_0 = 0$. Otherwise, α_0 can be determined from Equation 16-32 with M = 1. [A multiplying reference sample can also be used if it is sufficient to obtain relative correction factors (Ref. 35).]

Step 2: Now assay an unknown multiplying sample that requires a self-multiplication correction. This measurement yields R and T. If the sample is pure metal, $\alpha = 0$. If the sample is of the same composition as the small reference sample used in Step 1, then $\alpha = \alpha_0$. If the sample is pure plutonium oxide, then from Tables 11-1 and 11-3 it is possible to calculate

$$\alpha = \frac{13\,400\,f_{238} + 38.1\,f_{239} + 141\,f_{240} + 1.3\,f_{241} + 2.0\,f_{242} + 2690\,f_{\text{Am-241}}}{1020\,(2.54\,f_{238} + f_{240} + 1.69\,f_{242})} \qquad (16\text{-}35)$$

if the isotopic fraction f of each plutonium isotope and of ^{241}Am is known. Equation 11-7 can be used to correct the calculated value of α for the presence of major impurities that have high (α,n) cross sections if the concentrations of these impurities are known. For inhomogeneous or poorly characterized plutonium oxide, scrap, or waste where α cannot be determined by one of the above methods, this self-multiplication correction cannot be used.

Step 3: Calculate the ratio

$$r = \frac{R/T}{R_0/T_0}\,\frac{(1+\alpha)}{(1+\alpha_0)} \qquad (16\text{-}36)$$

This ratio will be larger than 1 for multiplying samples with M > 1 because sample self-multiplication increases R more than T. The ratio r is independent of detector efficiency, die-away time, and coincidence gate length. Note that all count rates in Equation 16-36 should be corrected for background and electronic deadtimes.

Step 4: The leakage multiplication M is given by

$$2.062(1 + \alpha)M^2 - [2.062(1 + \alpha) - 1]M - r = 0 \ . \qquad (16\text{-}37)$$

Equation 16-37 can be derived from Equations 16-33 and 16-34 (Refs. 36 and 37).

Step 5: The coincidence counting correction factor for self-multiplication CF is Mr. To summarize,

$$\begin{aligned} &T(\text{corrected for mult.}) = T/M \\ &R(\text{corrected for mult.}) = R/Mr \ . \end{aligned} \qquad (16\text{-}38)$$

This self-multiplication correction has no adjustable parameters and is geometry-independent. For example, suppose that two plutonium samples are brought closer and closer together. As this occurs, M will increase, the induced-fission chain lengths will increase, the mean effective multiplicity will increase, and R/T will increase. Equation 16-37 will yield larger values of M, and Equation 16-38 will automatically yield larger correction factors. Examples are given in Ref. 33 and in Figure 17.8.

When Equation 16-38 is used to linearize the calibration curve so that

$$m_{240} = R/kMr \ , \qquad (16\text{-}39)$$

then Equations 16-31, 16-36, and 16-39 require that the calibration constant k and the detector efficiency ε be related by

$$k = \varepsilon \nu_s(473/\text{s-g}) \frac{R_0}{T_0}(1 + \alpha_0) \ . \qquad (16\text{-}40)$$

This relation is not important in practice because k is usually obtained by calibration, but it may provide a diagnostic to indicate whether the detector efficiency or the small reference sample have been properly measured.

16.8.5 Applications and Limitations of the Simple Correction

Although the self-multiplication correction factors given by Equations 16-37 and 16-38 provide a complete correction with no adjustable parameters, the following assumptions were made in the derivation in order to obtain simple equations:

(1) It was assumed that detector efficiency was uniform over the sample volume. This is not always the case, but is becoming easier to realize with instruments such as the upgraded High Level Neutron Coincidence Counter (HLNCC-II) described in Section 17.2.3.

(2) It was assumed that (α,n) neutrons and spontaneous fission neutrons had the same energy spectra, so that the detection efficiency ε, fission probability p, and induced-fission multiplicity ν_I would be the same for both neutron sources. In general this is not the case, although for plutonium oxide the (α,n) and spontaneous fission neutrons have similar mean energies (2.03 MeV and 1.96 MeV, respectively) but different spectrum shapes.

(3) It was assumed that all fission chains are simultaneous within the die-away time of the detector. This is not true for neutrons that re-enter the sample from the detector (reflected neutrons)(Ref. 5).

These approximations introduce errors into the correction. Values for M given by Equation 16-37 may differ from values obtained from Monte Carlo codes. Values for the coincidence correction factor CF = Mr are usually better, presumably because some errors cancel in the use of ratios. The correction usually gives best fits of 2 to 3% to the data, which is good but is larger than the measurement relative standard deviation (on the order of 0.5%).

Applications of the simple self-multiplication correction are given in Table 16-2, columns 10 and 11, and in Figures 17.8, 17.19, 17.20 and 17.22 for plutonium oxide, metal, and nitrate solutions. Good results have been reported for plutonium oxide in Ref. 22, for plutonium metal in Refs. 33 and 36, and for breeder fuel-rod subassemblies in Ref. 38.

The above applications show that good results, typically 2 to 3%, can be obtained with the self-multiplication correction for well-characterized material despite the assumptions made in the derivation. However, the need to know α, the ratio of (α,n) to spontaneous fission neutrons, for each sample to be assayed poses a severe limitation on the applicability of the technique. For scrap, waste, impure oxide, or metal with an oxidized surface, α cannot be determined. Any error in the choice of α leads to an error of comparable size in the corrected assay value. In such cases the multiplication correction should be used only as a diagnostic for outliers. For many classes of oxide, where α may be somewhat uncertain but sample density and geometry are fixed, Krick (Ref. 39) has found that two-parameter calibration curves without self-multiplication corrections provide the best assay accuracy.

The fundamental limitation of the simple multiplication correction is that only two parameters are measured by each assay, R and T. The number of unknown variables is at least three: the sample mass, the sample self-multiplication, and the (α,n) reaction rate. Further improvements in multiplication corrections can be made if coincidence counters are built that provide a third measured parameter, such as triple coincidences (Refs. 23 and 33).

16.9 OTHER MATRIX EFFECTS

The dominant matrix effect in passive neutron coincidence counting is usually the self-multiplication process described in Section 16.8. If corrections for electronic count-rate losses and self-multiplication can be properly applied, the coincidence response is usually linear with sample mass. However, other matrix effects can affect the assay and may be overlooked at times. These effects are summarized in this section, which is based in part on Ref. 40.

1. (α,n) contaminants

For plutonium samples the most important (α,n) emitters are oxygen and fluorine. Fluorine concentrations of 10 to 400 ppm are typical, and oxygen (in water) may be as

high as several percent. The calculated effect of fluorine and water on the total neutron count rate is given in Section 14.2.3 of Chapter 14. Such (α,n) contaminants may bias the coincidence assay by a few percent. If their concentrations are known, the effects can be accounted for in the self-multiplication correction.

2. Hydrogen content

The hydrogen in water affects the neutron coincidence response by shifting the neutron energy spectrum (see Chapter 14, Section 14.2.4). This increases the detector efficiency and the sample self-multiplication. The former effect can be minimized by careful detector design, and the latter is taken into account by the multiplication correction.

3. Container wall effects

Neutron scattering and reflection by the container wall can increase detection efficiency and sample self-multiplication. An increase in the coincidence count rate up to 7% has been observed. Container effects can be estimated by measuring a californium source with and without an empty sample can.

4. Influence of uranium on plutonium assay

The addition of uranium to plutonium (as in mixed oxide) has the following effects: additional multiplication in ^{235}U; decrease in plutonium multiplication due to a "dilution" of the plutonium; and additional fast multiplication in ^{238}U. Despite different ^{239}Pu, ^{235}U, and ^{238}U fission multiplicities, the multiplication correction works well for mixed plutonium and uranium if there are no additional unknown (α,n) sources.

5. Neutron moderation and absorption (self-shielding)

In plutonium nitrate solutions, moderation leading to increased neutron absorption has been observed (Chapter 17, Section 17.2.7). In active coincidence counting of uranium, neutron absorption and self-multiplication are both strong and opposing effects. The presence of both effects often yields nearly straight calibration curves (Chapter 17, Figures 17.24 and 17.29).

6. Neutron poisons

Boron, cadmium, and some other elements have high thermal-neutron capture cross sections and can absorb significant numbers of neutrons. Problems with neutron poisons have been observed in the active assay of fresh light-water-reactor fuel assemblies.

7. Sample geometry

If the detection efficiency is not uniform over the sample volume, then the coincidence response can vary with sample geometry. Passive counters are now usually designed so that the whole sample will be in the region of uniform efficiency. For active coincidence counters, the source-to-sample distance is very important, and consistent positioning of samples is essential.

8. Sample density

Variations in plutonium oxide density due to settling or shaking during shipping and handling can affect the passive coincidence response by as much as 10%.* The multiplication correction can take these variations into account for samples of similar composition if the samples are within the detector's uniform efficiency region. For active coincidence counting, density variations affect both self-multiplication and self-shielding. No correction is available.

9. Scrap and waste matrices

Here it is helpful to know what the matrix is and to know which of the above-mentioned effects might be present. For plutonium-bearing materials, the coincidence response is usually more reliable than the totals response, but may provide only an upper limit on the quantity of ^{240}Pu. In general, it is useful to measure both the totals and the coincidence response and to use the totals response or the coincidence/totals ratio as a diagnostic to help interpret the coincidence response.

REFERENCES

1. M. S. Krick, "^{240}Pu-effective Mass Formula for Coincidence Counting of Plutonium with Shift Register Electronics," in "Nuclear Safeguards Program Status Report, May—August 1977," J. L. Sapir, Comp., Los Alamos Scientific Laboratory report LA-7030-PR (1977), p. 16.

2. C. H. Westcott, "A Study of Expected Loss Rates in the Counting of Particles from Pulsed Sources," *Royal Society of London,* A194 (1948).

3. C. H. Vincent, "The Pulse Separation Spectrum for the Detection of Neutrons from a Mixture of Fissions and Single-Neutron Events," *Nuclear Instruments and Methods* 138, 261 (1976).

4. N. Pacilio, "Reactor Noise Analysis in the Time Domain," AEC Critical Review Series TID 24512 (1969).

*Private communication from F. J. G. Rogers, Harwell, United Kingdom, 1984.

5. K. Boehnel, "Determination of Plutonium in Nuclear Fuels Using the Neutron Coincidence Method," KFK2203, Karlsruhe, 1975, and AWRE Translation 70 (54/4252), Aldermaston, 1978.

6. J. Jacquesson, *Journal of Physics* 24, Supp. to No. 6, 112A (1963).

7. G. Birkhoff, L. Bondar, and N. Coppo, "Variable Deadtime Neutron Counter for Tamper-Resistant Measurements of Spontaneous Fission Neutrons," Eurochemic Technical Report EUR-4801e (1972).

8. K. Lambert and J. Leake, "A Comparison of the VDC and Shift Register Neutron Coincidence Systems for ^{240}Pu Assay," *Nuclear Materials Management* VII (4), 87 (1979).

9. W. Stanners, "Brief Note on Analysis of VDC Results," Commission of the European Communities, Luxembourg, CEL-DXIII-E (1977).

10. N. Ensslin, M. Evans, H. Menlove, and J. Swansen, "Neutron Coincidence Counters for Plutonium Measurements," *Nuclear Materials Management* VII (2), 43 (1978).

11. A. Prosdocimi and P. Hansen, "Evaluation of the Physical Performances of Neutron Variable Deadtime Counters, Part II—Neutron Physics," Joint Research Centre report FMM/64 (1981).

12. E. W. Lees and B. W. Hooten, "Variable Deadtime Counters, Part III: A Critical Analysis," Atomic Energy Research Establishment report R9701 (1980).

13. C. V. Strain, "Potential and Limitations of Several Neutron Coincidence Equipments," Naval Research Laboratory memorandum 2127 (1970).

14. R. Sher, "Operating Characteristics of Neutron Well Coincidence Counters," Brookhaven National Laboratory report 50332 (1972).

15. E. J. Dowdy, C. N. Henry, A. A. Robba, and J. C. Pratt, "New Neutron Correlation Measurement Techniques for Special Nuclear Material Assay and Accountability," International Atomic Energy Agency report IAEA-SM-231/69 (1978).

16. E. J. Dowdy, G. E. Hansen, A. A. Robba, and J. C. Pratt, "Effects of (α,n) Contaminants and Sample Multiplication on Statistical Neutron Correlation Measurements," Proc. 2nd Annual ESARDA Symp. on Safeguards and Nuclear Material Management, Edinburgh, U.K., March 26-29, 1980.

17. A. Robba, E. Dowdy, and H. Atwater, "Neutron Multiplication Measurements Using Moments of the Neutron Counting Distribution," *Nuclear Instruments and Methods* 215, 473 (1983).

18. K. V. Nixon, E. Dowdy, S. France, D. Millegan, and A. Robba, "Neutron Multiplication Measurement Instrument," *IEEE Transactions on Nuclear Science* NS-30 (1) (1983).

19. M. Stephens, J. Swansen, and L. East, "Shift Register Neutron Coincidence Module," Los Alamos Scientific Laboratory report LA-6121-MS (1975).

20. J. Swansen, N. Ensslin, M. Krick, and H. Menlove, "New Shift Register for High Count Rate Coincidence Applications," in "Nuclear Safeguards Research Program Status Report, September—December 1976," J. L. Sapir, Comp., Los Alamos Scientific Laboratory report LA-6788-PR (June 1977), p. 4.

21. J. Swansen, P. Collinsworth, and M. Krick, "Shift Register Coincidence Electronics System for Thermal Neutron Counters," *Nuclear Instruments and Methods* 176, 555 (1980).

22. K. Lambert, J. Leake, A. Webb, and F. Rogers, "A Passive Neutron Well Counter Using Shift Register Coincidence Electronics," Atomic Energy Research Establishment report 9936 (1982).

23. M. Krick and J. Swansen, "Neutron Multiplicity and Multiplication Measurements," *Nuclear Instruments and Methods* 219, 384 (1984).

24. M. Krick and H. Menlove, "The High-Level Neutron Coincidence Counter User's Manual," Los Alamos Scientific Laboratory report LA-7779-M (1979).

25. M. S. Krick, "Calculations of Coincidence Counting Efficiency for Shift-Register and OSDOS Coincidence Circuits," in "Nuclear Safeguards Research and Development Program Status Report, May—August 1977," Los Alamos Scientific Laboratory report LA-7030-PR (1978), p. 14.

26. J. Swansen and N. Ensslin, "A Digital Random Pulser for Testing Nuclear Instrumentation," *Nuclear Instruments and Methods* 188, 83 (1981).

27. E. Adams, "Deadtime Measurements for the AWCC," Los Alamos National Laboratory memorandum Q-1-82-335 to H. Menlove (April 29, 1982).

28. J. Swansen and N. Ensslin, "HLNCC Shift Register Studies," in "Nuclear Safeguards Research and Development Program Status Report, April—June 1980," G. R. Keepin, Ed., Los Alamos Scientific Laboratory report LA-8514-PR (February 1981), p. 11.

29. C. H. Vincent, "Optimization of the Neutron Coincidence Process for the Assay of Fissile Materials," *Nuclear Instruments and Methods* 171, 311 (1980).

30. H. Menlove, J. Swansen, and E. Adams, "Coincidence Counting Deadtime Study," Los Alamos National Laboratory memorandum Q-1-83-461 (June 27, 1983).

31. J. E. Swansen, "Deadtime Reduction in Thermal Neutron Coincidence Counters," Los Alamos National Laboratory report LA-9936-MS (March 1984).

32. H. O. Menlove, "Description and Operation Manual for the Active Well Coincidence Counter," Los Alamos Scientific Laboratory report LA-7823-M (1979), p. 25.

33. N. Ensslin, J. Stewart, and J. Sapir, "Self-Multiplication Correction Factors for Neutron Coincidence Counting," *Nuclear Materials Management* VIII (2), 60 (1979).

34. K. Boehnel, "The Effect of Multiplication on the Quantitative Determination of Spontaneously Fissioning Isotopes by Neutron Correlation Analysis," *Nuclear Science and Engineering*, 90, 75-82 (1985).

35. M. T. Swinhoe, "Multiplication Effects in Neutron Coincidence Counting: Uncertainties and Multiplying Reference Samples," U.K. Atomic Energy Commission report AERE-R 11678, Harwell, March 1985.

36. N. Ensslin, "A Simple Self-Multiplication Correction for In-Plant Use," Proc. 7th ESARDA Symposium on Safeguards and Nuclear Material Management, Liege, Belgium, 21-23 May 1985.

37. W. Hage and K. Caruso, "An Analysis Method for the Neutron Autocorrelator with Multiplying Samples," Joint Research Centre, Ispra, Italy, report EUR 9792 EN (1985).

38. G. Eccleston, J. Foley, M. Krick, H. Menlove, P. Goris, and A. Ramalho, "Coincidence Measurements of FFTF Breeder Fuel Subassemblies," Los Alamos National Laboratory report LA-9902-MS (1984).

39. M. S. Krick, "Neutron Multiplication Corrections for Passive Thermal Neutron Well Counters," Los Alamos Scientific Laboratory report LA-8460-MS (1980).

40. M. S. Krick, R. Schenkel, and K. Boehnel, in "Progress in Neutron Coincidence Counting Techniques," report of the IAEA Advisory Group Meeting, Vienna, Austria, 7-11 October 1985, IAEA Dept. of Safeguards General Report STR-206.